



Iranian Research Organization  
for Science and Technology  
(IROST)

Advances  
Environmental  
Technology



Journal home page: <https://aet.irost.ir/>

# A Comparative study on photocatalytic degradation of quinalphos pesticide using ZnO/MgO and ZnO/SnO<sub>2</sub> nanocomposites

S. Sibmah Stalin\*, E.K. Kirupa Vasam Jino

Department of Chemistry and Research Centre, Nesamony Memorial Christian College, Tamilnadu, India

## ARTICLE INFO

Document Type:  
Research Paper

Article history:  
Received 20 July 2022  
Received in revised form  
12 July 2023  
Accepted 15 July 2023

Keywords:  
Organic contaminants  
Quinalphos  
Nanocomposite  
Photocatalyst  
Photocatalytic degradation

## ABSTRACT

The photocatalytic degradation of Quinalphos, an organic pesticide, in the presence of modified ZnO metal composites, namely ZnO/MgO and ZnO/SnO<sub>2</sub>, was investigated at normal pH in the presence of sunlight. The structural and morphological properties of both the synthesized nanocomposites were characterised by different spectral techniques. The effect of pesticide concentration, catalyst dosage, and pH on the photocatalytic degradation efficiency was investigated. The photocatalytic activity of the respective nanocomposites on the degradation of Quinalphos was confirmed by UV-Visible spectroscopy. Moreover, the recycling ability of the prepared nanocomposites was also conducted and analyzed. However, the photocatalytic efficiency of ZnO/SnO<sub>2</sub> nanocomposite was more efficient than the ZnO/MgO nanocomposite for the treatment of pesticide effluent, achieving 98 % and 95 % of total organic carbon (TOC) and chemical oxygen demand (COD) removals, respectively. The present study therefore concluded that the ZnO/SnO<sub>2</sub> nanocomposite was the more stable and well organised composite, which could be the preferred treatment of industrial and agricultural wastewater containing organic contaminants within a short span of time.

## 1. Introduction

Water pollution created by pesticide contaminants has exploited the affluence of the environment, giving rise to several health problems for humans and aquatic organisms [1]. The uncontrolled usage of pesticides in agriculture and their application in paper, leather, paint, and wood conservation units has created acute contamination and degradation in water quality. Organophosphate pesticides are

applied extensively in agriculture to enrich the yield of food grains and protect crops from pests [2]. Quinalphos is one of the powerful organophosphate pesticides utilised for the conservation and high productivity of vegetables, tea, cotton, and fruits. Besides their advantages, the incessant usage of this chemical pesticide in agriculture has negatively impacted property, productivity, and the texture of the ecosystem [3]. Quinalphos is readily soluble in water; hence, it is

\*Corresponding author

E-mail: sibmah1998@gmail.com

DOI:10.22104/AET.2023.5769.1583

COPYRIGHTS: ©2023 Advances in Environmental Technology (AET). This article is an open access article distributed under the terms and conditions of the Creative Commons Attribution 4.0 International (CC BY 4.0) (<https://creativecommons.org/licenses/by/4.0/>)

easily transported through the soil and contaminates the underground water streams. Moreover, this organic pollutant stays in aqueous media for a long time, contaminating the groundwater even at very low concentrations [4]. Also, the availability of potable drinking water has been declining every day due to the contamination of this type of pesticide pollutants [5]. Hence, to improve the quality of water, there is a need for an instant remedy for the eradication of Quinalphos and its residues from water [6]. In recent times, several procedures, including physical absorption, biological degradation, etc., have evolved for the eradication of organic pollutants [7]. However, ordinary treatment processes cannot eliminate these pesticide effluents [8]. Hence, a very effective, energetic, and eco-friendly method is required to eliminate these pollutants. Among the various advanced water treatment methods, photocatalytic degradation has been proclaimed as an efficacious, affordable, and environmentally friendly process [9]. Moreover, this method is regarded as a boosting technology for the treatment of water contaminants [10]. Among the various natural energy resources, solar energy is regarded to be the most efficient, readily available, and renewable energy source on Earth [11]. Furthermore, solar irradiation has been utilised to transform pollutants from convoluted compounds to uncomplicated and harmless molecules, avoiding the need for further treatment and disposal of by-products [12]. The photocatalytic degradation method presents a sparing and satisfying feasible solution for the treatment of organic contaminants present in water [13]. Photocatalyst metal oxide nanoparticles and their composite materials have received extensive attention in recent times owing to their catalytic activity [14,15]. They have been extensively applied for the degradation of pollutants present in local and industrial water streams [16]. Semi-conductor modified nanocomposites are highly photosensitive and possess effective charge transporting capacity [17,18]. Consequently, they can be applied in environmental remediation for the treatment of pollutants present in water [19,20,21]. Zinc oxide is a semiconductor that is applied widely for the degradation of organic pollutants due to its excellent chemical stability, low fabrication cost,

low toxicity, and other advantages [22]. Kaur et al. studied the degradation of Quinalphos using ZnO and TiO<sub>2</sub> nanoparticles under UV light for four hours. According to their analysis, TiO<sub>2</sub> performed better catalytic activity than ZnO [23]; the activity of ZnO was hindered by its band gap energy and the recombination of electron hole pairs [24]. In order to maximise its capacity as a semiconductor in photocatalytic usage zinc oxide was doped with other metal oxides. Thus, the present study attempted to modify zinc oxide with magnesium oxide and tin oxide to construct ZnO/MgO and ZnO/SnO<sub>2</sub> nanocomposites. Magnesium oxide is a promising inorganic material widely used in many applications such as sensors, water treatment, catalysis, and adsorbents. This is mainly due to their superior surface reactivity and chemical and thermal stability [25]. Tin oxide has been found to be a powerful photocatalyst for the degradation of organic pollutants in aqueous solution due to its excellent properties, such as transparency, good chemical stability, low cost, and eco-friendly character [26]. Only a few works have been reported regarding the degradation of Quinalphos; the decomposition of Quinalphos consumes more time with low degradation efficiency. Sraw et al. reported 98.09% of Quinalphos degradation in 180 minutes [27]. Lingaraj et al. studied the degradation of Quinalphos under visible light using a mercury vapour lamp for 90 minutes [28]. Renuga et al. exposed 84% degradation of Quinalphos using ZnO/GO in 45 minutes under UV light [29]. Nidhi et al. reported 87.5% of Quinalphos degradation in 240 minutes using Mn-N-Co doped TiO<sub>2</sub> under visible light [30].

In the current study, ZnO/MgO and ZnO/SnO<sub>2</sub> nanocomposites were fabricated and applied for the degradation of Quinalphos with the objective of comparing their photocatalytic performance. Zinc acetate, magnesium chloride, ammonium hydroxide, and tin chloride were used as precursors for synthesizing the ZnO/MgO and ZnO/SnO<sub>2</sub> nanocomposites. The surface morphology, crystal structure, and properties of the prepared materials were examined by using different analytical techniques: X-ray (XRD), Ultra-violet (UV), Scanning Electron Microscopy (SEM), Energy Dispersive X-Ray EDX, and Fourier-Transform Infrared (FT-IR) analysis. Moreover, the

effect of pesticide concentration, photocatalyst dosage, pH, and recycling ability of the prepared nanocomposites was analysed and their performance in degradation was compared. Fernandez et al. described an 87% degradation of methylene blue for 60 minutes under UV irradiation in the presence of a ZnO/MgO photocatalyst [31]. Sangeetha et al. declared a 78% degradation of IC dye using ZnO/MgO in the exposure to UV light for an irradiation time of about 90 minutes [32]. Zarei et al. observed only a 70% degradation of methylene blue in the presence of ZnO/SnO<sub>2</sub> nanocomposite film under ultraviolet irradiation [33]. Naveen et al. reported a 78% degradation of cibacron red dye under ultraviolet irradiation for 120 minutes [34]. After a deliberated review of the literature, earlier studies reported that ZnO/MgO and ZnO/SnO<sub>2</sub> nanocomposites could degrade the organic contaminants only under UV light irradiation, and the time required for the same was greater. Hence, the purpose of this current work is to introduce a fast, economical, and energy efficient solution to treat organic contaminants present in water. In most of the published literature, the experiments were performed at a high pH (test solution), but eco-friendly pH under natural sunlight was used in the current study.

## 2. Materials and methods

All the chemicals were of analytical grade. The chemicals were utilised as received without further purification. Zinc acetate dihydrate [Zn(CH<sub>3</sub>CO<sub>2</sub>)<sub>2</sub>·2H<sub>2</sub>O] and magnesium chloride (MgCl<sub>2</sub>) were purchased from Nice laboratories, Maharashtra (India). Ammonium hydroxide (NH<sub>4</sub>OH) was purchased from Iso-chem Laboratories, Kochi (India). Tin chloride (SnCl<sub>2</sub>) was purchased from Reachem Laboratory Chemicals pvt, Ltd, Chennai (India).

### 2.1. Synthesis of modified ZnO nanocomposites

The nanocomposite was prepared using zinc acetate, graphite powder, and copper sulphate as precursors.

#### 2.1.1. Synthesis of ZnO/MgO nanocomposite

The ZnO/MgO nanocomposite was synthesised by dissolving a known quantity of zinc acetate dehydrate and magnesium chloride in 100 mL of double distilled water. A calculated amount of

ammonium hydroxide solution was added drop wise to the above suspension, and stirring was continued for about 4 h. The supernatant liquid was discarded and centrifuged. The obtained precipitate was dried on a hot plate at 80 °C and crushed in an agate mortar pestle to obtain the ZnO/MgO nanocomposite [35].

#### 2.1.2. Synthesis of ZnO/SnO<sub>2</sub> nanocomposite

A known quantity of zinc acetate and tin chloride was dissolved in 100 mL of double distilled water. A calculated amount of 1:1 (v/v) ammonia solution was added drop wise to the above suspension with continuous stirring for 2 h. The precipitate was kept without any interruption for 12 hours at room temperature. The resulting products were filtered and dried in an air oven at 80 °C for 2 hours. Finally, the prepared composite was calcined at 300 °C for 2 h to obtain the ZnO/SnO<sub>2</sub> nanocomposite [34].

## 3. Characterisation of nanocomposite

The structural and crystalline phase of the sample was recognised using a Bruker D8 advance XRD with Cu-K $\alpha$  radiation 40 mA with a scanning rate of 2° min<sup>-1</sup>. The morphology and structural analysis of the composites was examined using Scanning Electron Microscope (model Jeol 5800LV). The elemental composition was analysed using Energy Dispersive X-ray spectrometry (EDS) analysis (model JSM-7100F). The FT-IR analysis of the nanocomposite was studied using a Bruker Invenio spectrometer, and the diffuse reflectance absorption spectra (DRS) were recorded on JASCO equipment in the range of 200-2500 nm.

### 3.1. X-ray diffraction analysis

The X-ray diffraction analysis is a non-destructive methodology suited to examine the crystalline structure of materials. Figure 4A and Figure 4B show a standard XRD pattern of the ZnO/MgO and ZnO/SnO<sub>2</sub> nanocomposites, respectively. In Figure 1A, the diffraction peaks located at 31.93°, 34.54°, 36.33°, 47.68°, 56.82°, 68.17°, and 69.16° (JCPDS card no: 36-1451) designate the presence of the hexagonal phase of the zinc oxide lattice [36]. Moreover, the diffraction peaks at 36.41°, 42.96°, 56.82°, and 63.01° (JCPDS card no: 45-09646) specify the existence of a cubic phase of magnesium oxide [37]. Using the Debye Scherrer formula, the average crystal size of the ZnO/MgO

nanocomposite was evaluated to be 32 nm. In Figure 1B, the diffraction peaks at  $34.29^\circ$ ,  $49.05^\circ$ ,  $58.33^\circ$ , and  $62.96^\circ$  (JCPDS card no: 36-1451) relatively designate the presence of zinc oxide, whereas the diffraction peaks located at  $27.74^\circ$ ,  $34.29^\circ$ ,  $42.91^\circ$ ,  $49.05^\circ$ , and  $58.33^\circ$  specify the tetragonal rutile phase of tin oxide, respectively (JCPDS card no: 39-0511) [38]. This rutile phase in the ZnO/SnO<sub>2</sub> nanocomposite improved the employment of photo generated charge carriers. Hence, the organic contaminants can be degraded easily within a short span of time [39]. Moreover, the small size and large specific surface area of the ZnO/SnO<sub>2</sub> catalyst gave a favourable contribution towards high photocatalytic degradation activity. The average size of the prepared ZnO/SnO<sub>2</sub> nanocomposite was evaluated to be 28 nm.

### 3.2. SEM analysis

The surface morphology of the synthesised nanocomposites was ascertained through SEM analysis as shown in Figure – 2A and 2B. The ZnO/MgO nanocomposite revealed a flake like morphology, whereas the particles in the ZnO/SnO<sub>2</sub> nanocomposite were rough and possessed spherical morphology with less agglomeration [40,41]. The morphology of the ZnO/SnO<sub>2</sub> nanocomposite provided drastic charge separation

efficiency for this composite and thus showed an effective photocatalytic performance towards pollution degradation.

### 3.3. EDX analysis

In order to authorise the purity of the prepared ZnO/MgO and ZnO/SnO<sub>2</sub> nanocomposites, the EDX interpretation was analysed, as shown in Figure 3. The attributing peaks shown in Figure 3 (A) represent zinc, magnesium, and oxygen, but there are no additional peaks, further certifying the purity of the synthesized ZnO/MgO nanocomposite. The weight percentage of magnesium, zinc, and oxygen was found to be 33.54, 42.05, and 24.41, respectively. And this indicated that the prepared nanocomposite was composed only of zinc, magnesium, and oxygen without any other foreign elements. In Figure 3(B), the purity of the prepared ZnO/SnO<sub>2</sub> sample was certified by the attributing peaks representing zinc, tin, and oxygen, but there are no additional peaks, which further represented the purity of the synthesized ZnO/SnO<sub>2</sub> nanocomposite. The weight percentage of tin, zinc, and oxygen was 21.59, 50.61, and 27.80, respectively.

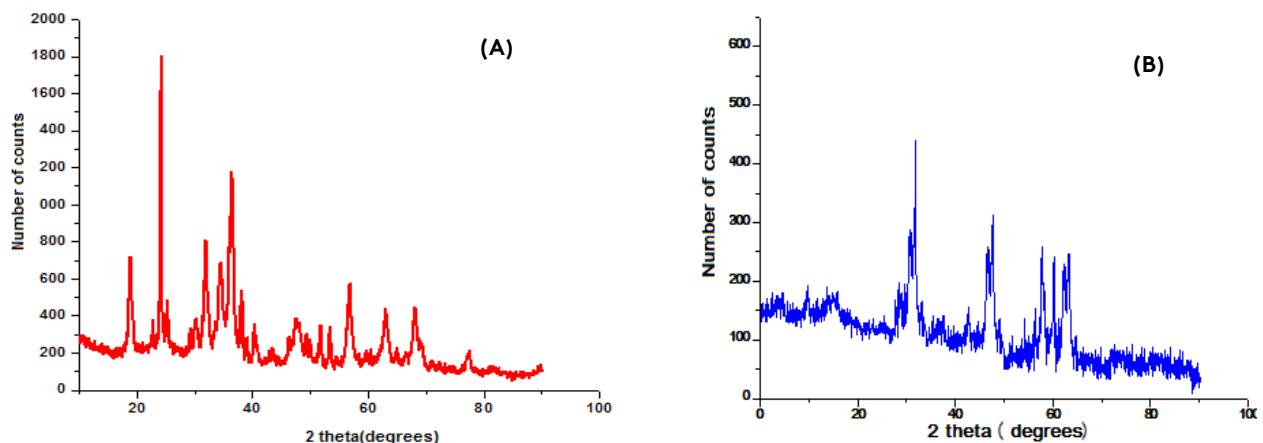


Fig. 1. XRD pattern of (A) ZnO/MgO nanocomposite (B) ZnO/SnO<sub>2</sub> nanocomposite.

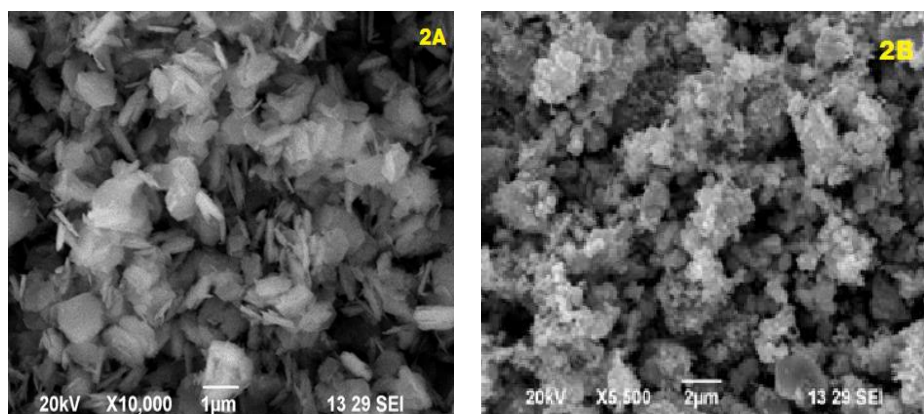


Fig. 2. SEM image of (A) ZnO/MgO nanocomposite (B) ZnO/SnO<sub>2</sub> nanocomposite.

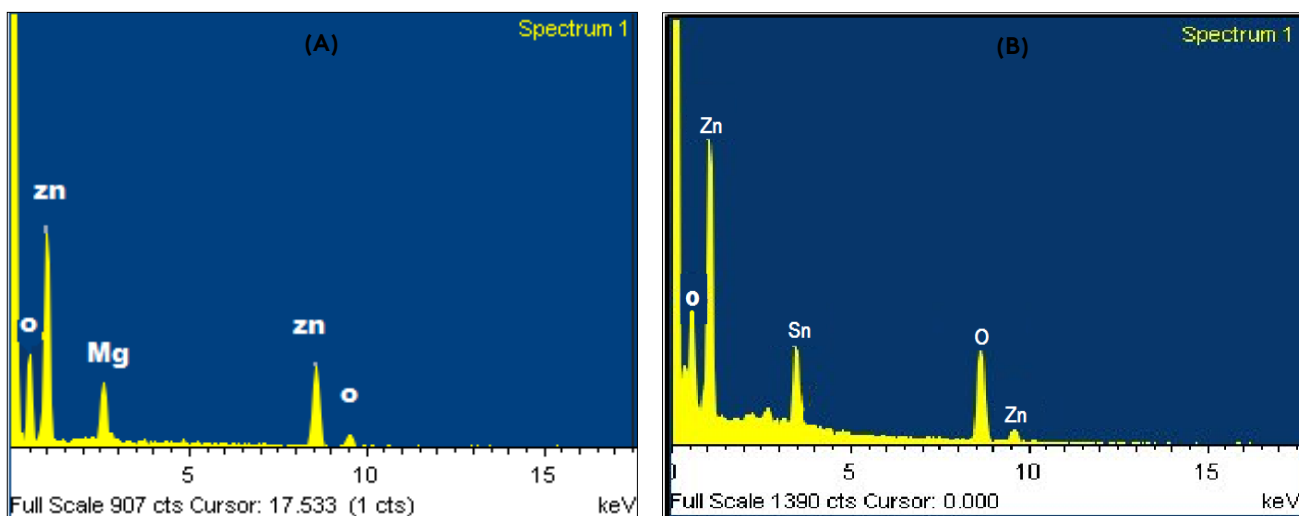


Fig.3. EDX pattern of (A) ZnO/MgO nanocomposite (B) ZnO/SnO<sub>2</sub> nanocomposite.

The atomic percentage of the synthesized nanocomposites together with the weight percentage was displayed in Table 1.

### 3.4. UV-Vis diffuse reflectance spectra (DRS) analysis

The optical properties of the prepared nanocomposites were investigated by UV-Vis diffuse reflectance spectra, as shown in Figures. 4A and 4B. The band gap energy of ZnO was 3.37 eV and hence it could not be excited by visible light under ambient conditions. In an attempt to magnify the photocatalytic activity of ZnO, it was coupled with MgO as well as SnO<sub>2</sub>. The performance of a photocatalyst strongly depends on its electronic band gap energy. For a photocatalyst to be active under visible light, its band gap energy should be smaller than 3 eV, which was achieved

for the synthesised ZnO/MgO and ZnO/SnO<sub>2</sub>. The band gap energy of the prepared ZnO/MgO nanocomposite was 2.78 eV and 2.25 eV for ZnO/SnO<sub>2</sub>. As the band gap energy of the ZnO/SnO<sub>2</sub> nanocomposite was smaller than the ZnO/MgO nanocomposite, the former was more dynamic.

Table 1. Elemental composition of ZnO/MgO and ZnO/SnO<sub>2</sub> nanocomposite.

Element	Weight percentage	Atomic percentage
Zinc	50.61	28.74
Tin	21.59	6.75
Oxygen	27.80	64.51

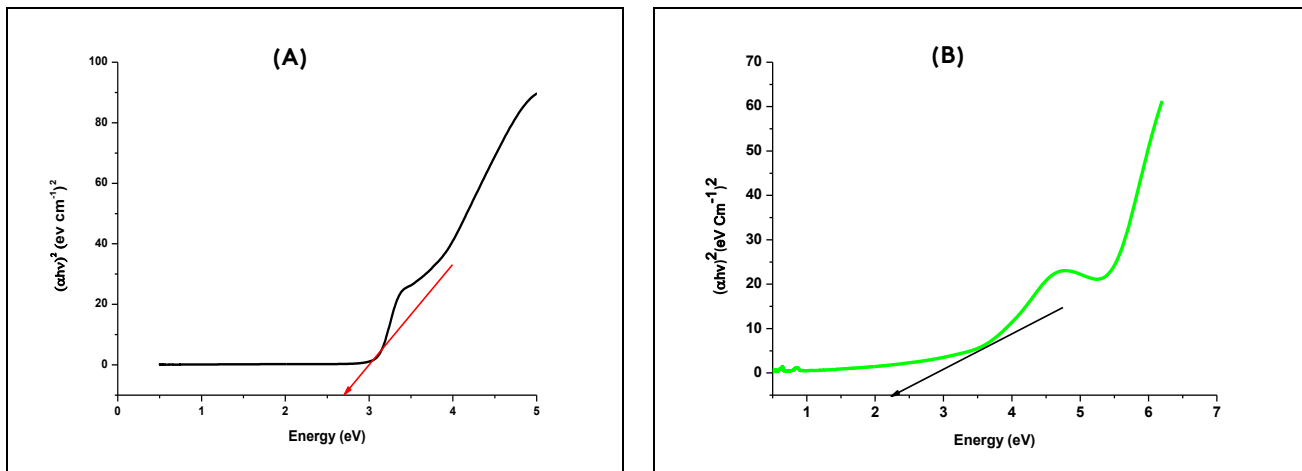


Fig. 4 UV-Vis DRS spectrum of (A) ZnO/MgO nanocomposite (B) ZnO/SnO<sub>2</sub> nanocomposite.

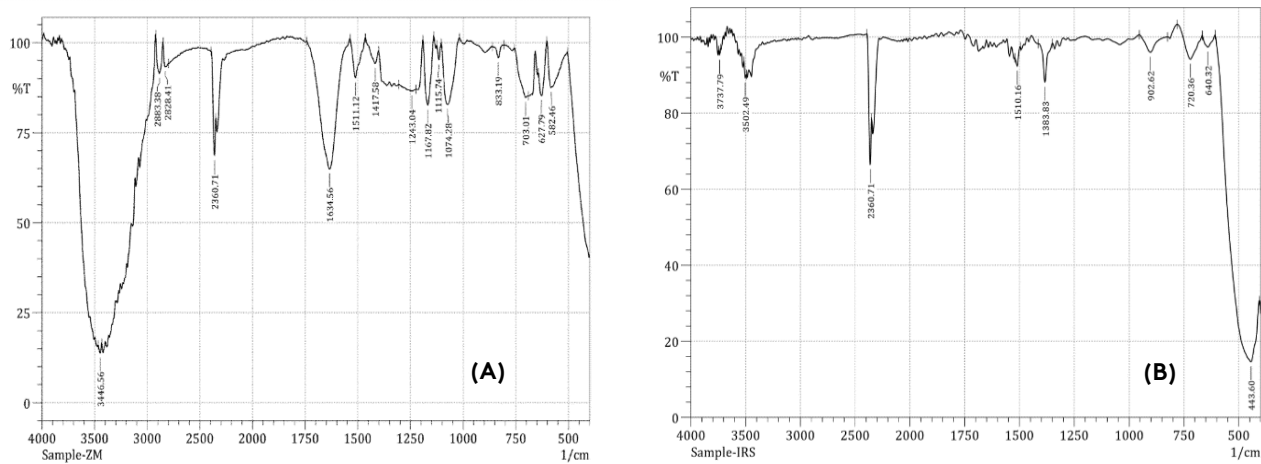


Fig.5. FT-IR spectrum of (A) ZnO/MgO nanocomposite (B) ZnO/SnO<sub>2</sub> nanocomposite.

### 3.5. FT-IR analysis

FT-IR studies were carried out to establish the functional groups and chemical bonds present in the metal oxide nanocomposites [42]. In the ZnO/MgO nanocomposite, the peak at 580  $\text{cm}^{-1}$  and 827  $\text{cm}^{-1}$  was due to the presence of Zn-O and Mg-O bonds, which assured the formation of a pure and composite form of the respective nanocomposite [43]. The peak at 1417  $\text{cm}^{-1}$  and 2883  $\text{cm}^{-1}$  was characteristic of the metal carbonyl group and residual organic components, respectively [35]. Further, a broad peak at 3446  $\text{cm}^{-1}$  corresponded to the primary alcoholic O-H functional group [44,45]. For the ZnO/SnO<sub>2</sub> nanocomposite, the origin of a well-defined band at 443  $\text{cm}^{-1}$  indicated the presence of pure zinc oxide [46]. A strong peak at 640  $\text{cm}^{-1}$  was attributed to the vibration of the O-Sn-O bond in ZnO/SnO<sub>2</sub> nanocomposite, as reported in the

literature [47]. The band at 2380  $\text{cm}^{-1}$  represented the stretching vibration of the C-H bonds. Finally, the absorbance at 3737  $\text{cm}^{-1}$  corresponded to the stretching vibration of hydroxyl group.

## 4. Photocatalytic Experiment

In order to analyse the photocatalytic performance of the prepared nanocomposites (ZnO/SnO<sub>2</sub> and ZnO/MgO) possessing different chemical compositions in the photocatalytic degradation of Quinalphos, the same doses of the synthesized nanocomposites were introduced into an aqueous solution containing 30 ppm of organic pesticide and Quinalphos as the contaminant at a neutral pH; the experiments were carried out separately for each nanocomposite. The solution was kept in the dark with stirring for about 30 minutes to establish an adsorption-desorption equilibrium. Then, the

whole experimental setup was kept in sunlight, and the stirring was continued. The degradation of Quinalphos was monitored by sampling 3mL of the test solution at regular intervals after irradiation, followed by centrifugation [48]. The concentration of the solution was analysed using a UV-visible spectrophotometer by monitoring the absorbance at 230 nm. A visual representation of photocatalytic degradation experiment was shown in Figure 6. The percentage of degradation efficiency of Quinalphos was calculated as follows:

$$\text{efficiency of degradation (\%)} = \frac{C_0 - C}{C_0} \times 100$$

where  $C_0$  is the initial concentration of the test solution and  $C$  is the concentration of the solution after photocatalytic degradation.

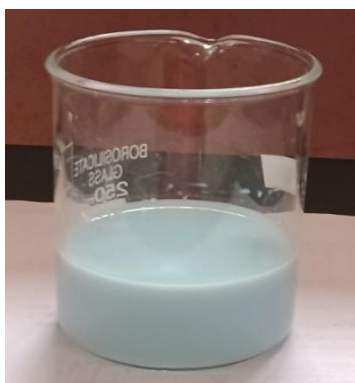
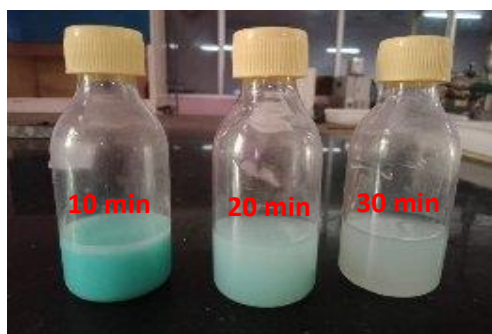
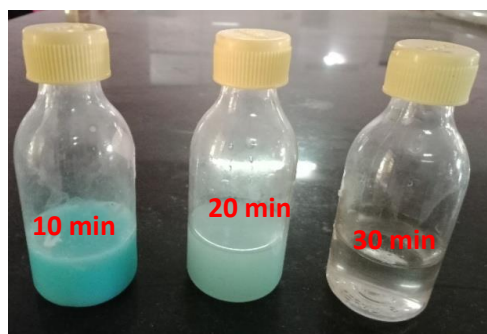


Fig. 6. Visual representation of photocatalytic degradation experimental solution before and after degradation.



(A)



(B)

Fig. 7. Visual observation for (A) ZnO/MgO degradation at 10, 20 and 30 minutes (B) Visual observation for ZnO/SnO<sub>2</sub> degradation at 10, 20, and 30 minutes.

## 6. Absorbance spectra measurements

Figures 8A and 8B show the evolution of the absorption spectra of the Quinalphos solution during the photocatalytic degradation experiments with the ZnO/MgO and ZnO/SnO<sub>2</sub> nanocomposites. The absorbance of the Quinalphos solution, i.e., 30

## 5. Photocatalytic degradation studies.

The results obtained from this examination displayed the excellent photocatalytic ability of the prepared photocatalysts for the degradation of Quinalphos under direct sunlight. The colour of the test solution turned from turbid pale blue to a colourless clear solution. The result of the experiments revealed that both ZnO/MgO and ZnO/SnO<sub>2</sub> nanocomposites showed very good degradation efficiency under visible light irradiation. The ZnO/MgO nanocomposite displayed 80% colour decay in 30 minutes (Figure 7A), whereas 100% of degradation was achieved by the ZnO/SnO<sub>2</sub> nanocomposite at 30 minutes of light irradiation (Figure 7B), indicating the degradation of Quinalphos pesticide.

ppm before and after irradiation, was monitored. The absorption maximum for the test solution at 230 nm was gradually decreased with irradiation time. The results of degradation revealed that the percentage of degradation with an irradiation time of 30 minutes using the ZnO/MgO and ZnO/SnO<sub>2</sub> nanocomposite was found to be 80 and

100, respectively. From the UV-Visible spectral analysis, it could be confirmed that ZnO coupled with SnO<sub>2</sub> degrade Quinalphos more briskly than ZnO/MgO nanocomposite.

### 7.2. Effect of photocatalyst loading

The degradation of pesticide depends on the adsorption of pesticide over the active sites on the surface of the photocatalyst, and only the adsorbed organic contaminant will undergo complete degradation. The photocatalytic degradation experiment was conducted over a range of catalyst amounts from 0.1 to 0.4 mg for the Quinalphos pesticide. The ZnO/SnO<sub>2</sub> nanocomposite showed the highest degradation of 100 % for 0.2 mg in 30 minutes. The degradation rate was less for the remaining doses of 0.1, 0.3, and 0.4 mg; for 0.4 mg of ZnO/MgO nanocomposite, it was recorded at 80% in 30

minutes. This is illustrated in Figures 10(A) and 10(B). However, compared to the ZnO/MgO nanocomposite, the ZnO/SnO<sub>2</sub> nanocomposite was more effective, as it showed better degradation efficiency. From the results of the XRD analysis, the potential of the ZnO/SnO<sub>2</sub> catalyst was higher due to its smaller size, larger surface area, and the presence of a sufficient number of surface-active sites on the catalyst. A further increase in the dosage of the photocatalyst generated more numbers of electron hole pairs, and the degradation of the pesticide molecules was induced due to the formation of more reactive radicals on the surface of the photocatalyst. Moreover, the increase in dynamic sites on the surface of catalyst was more accessible for the degradation to take place. Therefore, as the loading of the photocatalyst increased, photocatalytic degradation also increased.

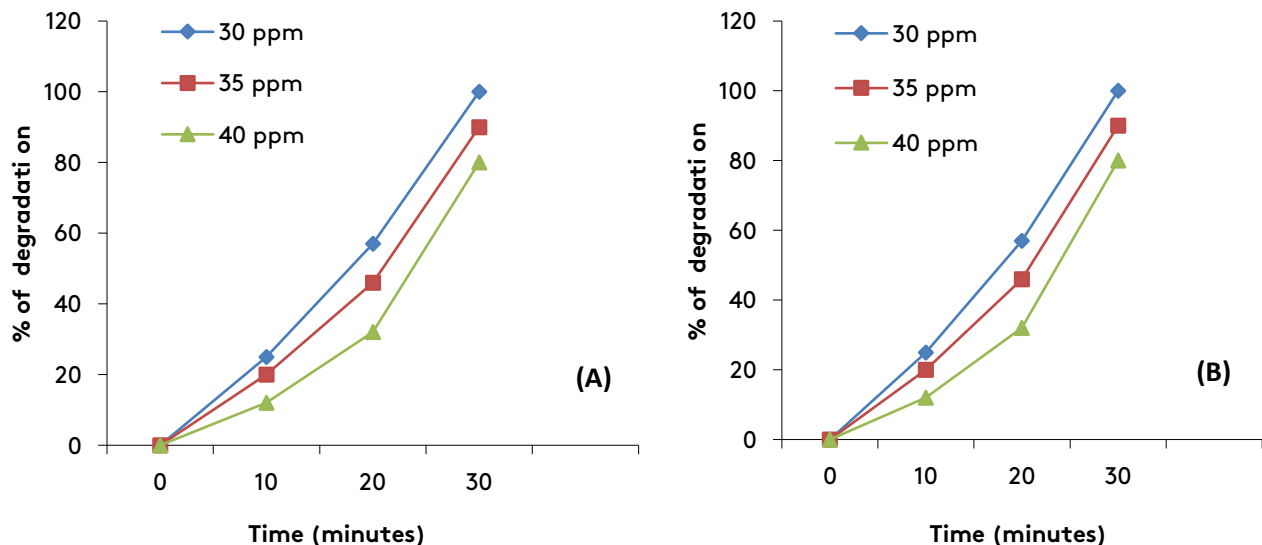


Fig.9. Effect of concentration of pesticide on (A) ZnO/MgO nanocomposite (B) ZnO/SnO<sub>2</sub> nanocomposite.



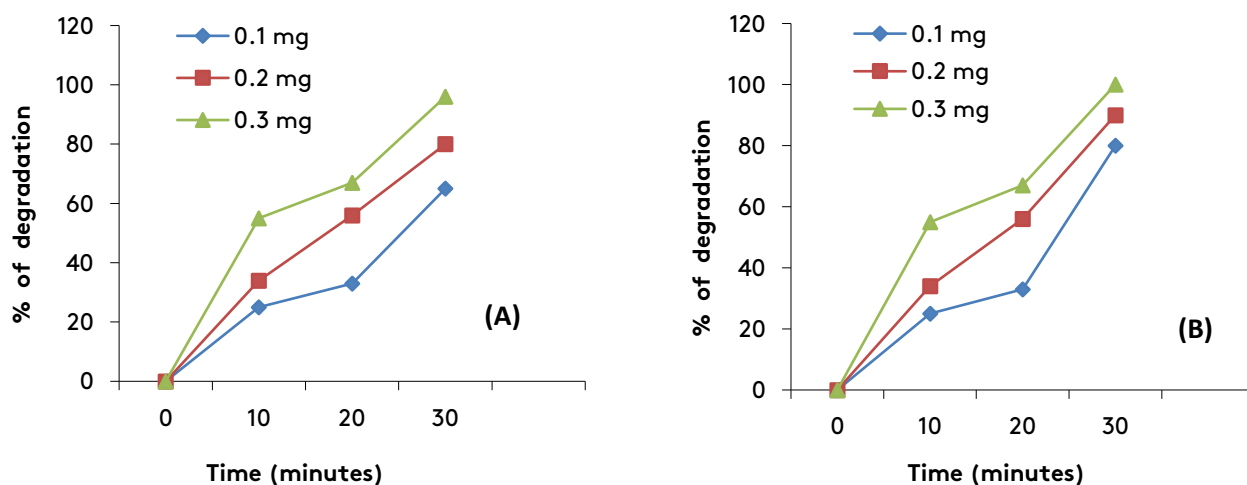


Fig.10. Effect of dosage of (A) ZnO/MgO nanocomposite (B) ZnO/SnO<sub>2</sub> nanocomposite.

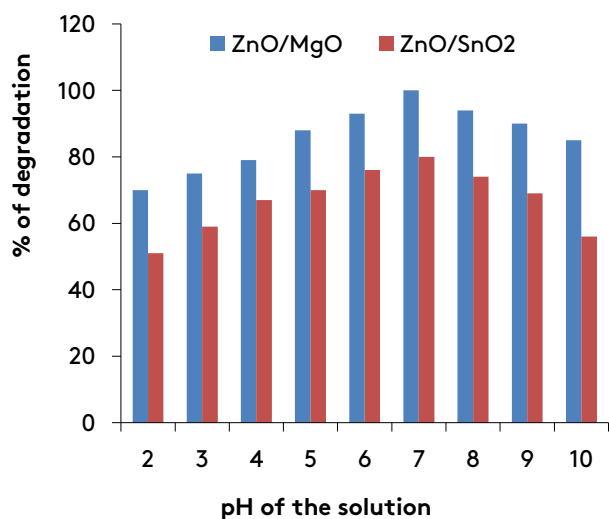


Fig.11. Effect of pH on ZnO/MgO and ZnO/SnO<sub>2</sub> nanocomposites.

### 7.3. Effect of pH

In order to study the effect of pH on the degradation potentiality of both the ZnO/MgO and ZnO/SnO<sub>2</sub> nanocomposites, the experiments were conducted in pH ranging from 2 to 10. The pH of the test solution was adjusted before irradiation using an HCl and NaOH solution. The percentage of degradation increased at an acidic pH and was reduced at basic pH, as shown in Figure 11. The ZnO/SnO<sub>2</sub> nanocomposite showed a maximum degradation of 100 % at pH 7, and the degradation efficiency was reduced to 85% at pH 10 in 30

minutes. However, the ZnO/MgO nanocomposite showed 80% degradation at pH 7 and decreased to 56% at pH 10 in 30 minutes. The current study revealed that both the ZnO/MgO and ZnO/SnO<sub>2</sub> nanocomposites have the capacity to degrade Quinalphos in acidic pH conditions.

### 8. Recycling ability of the composites

The recycling ability of the catalyst is very important for sustainable water treatment [49]. This capacity assures the stability of the catalyst [50]. In order to analyse the recycling ability of the prepared nanocomposites, the specified nanocomposite was accumulated by centrifugation from the test solution after the complete degradation of Quinalphos. The reclaimed nanocomposite was washed, filtered, dried, and employed for the next degradation cycle of the Quinalphos pesticide. This procedure was repeated for more cycles, and the degradation efficiency of Quinalphos remained the same for five cycles for ZnO/MgO and multiple cycles for the ZnO/SnO<sub>2</sub> nanocomposite, which was authenticated from the UV-Visible absorbance data. This was considered as a significant character of the ZnO/SnO<sub>2</sub> nanocomposite. From this outcome, it could be concluded that the ZnO/SnO<sub>2</sub> nanocomposite was more stable, eminent, and exposed a marvellous performance in its photocatalytic activity for degrading Quinalphos.

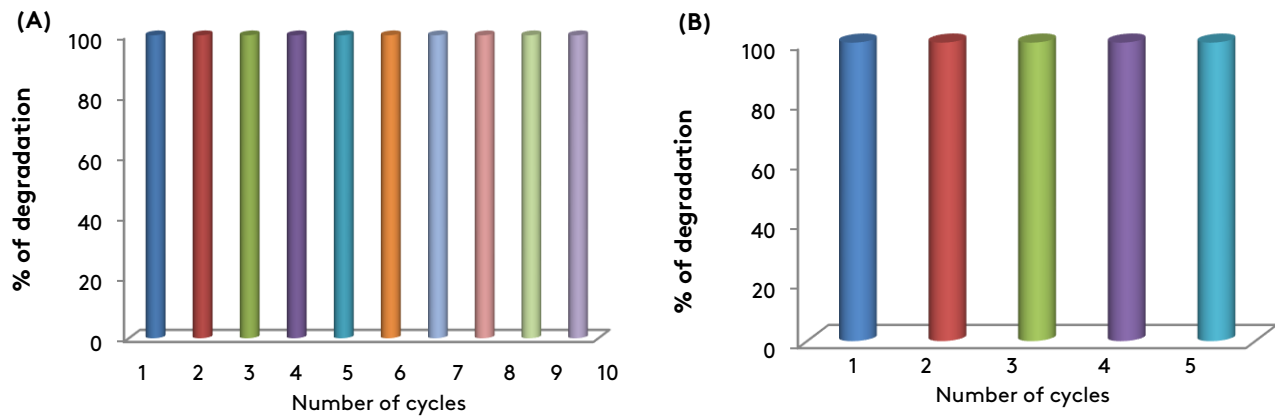


Fig.12. Recycling ability of (A) ZnO/SnO<sub>2</sub> nanocomposite (B) ZnO/MgO nanocomposite.

### 9. Chemical oxygen demand (COD) analysis

The marvellous photocatalytic performance of the ZnO/SnO<sub>2</sub> nanocomposite could also be evaluated by COD analysis. The initial and final COD value for the pesticide contaminant was found to be 11752 mg/L and 178 mg/L, respectively. The decrease in the COD value of the degraded solution confirmed the mineralisation of the pesticide molecule in conjugation with the elimination of colour. Therefore, in the presence of the ZnO/SnO<sub>2</sub> nanocomposite, about 98 % of the total COD was reduced in thirty minutes of light irradiation.

### 10. Total Organic Carbon (TOC) Analysis

The TOC measurement revealed the disappearance of organic carbon in the Quinalphos solution. The results obtained from this analysis showed that about 95% of organic carbon was terminated from the Quinalphos solution, which was achieved by using the ZnO/SnO<sub>2</sub> nanocomposite through photo degradation in 30 minutes. From this evaluation, it was observed that the ZnO/SnO<sub>2</sub> nanocomposite was an efficient photocatalyst to mineralise pesticide pollutants in a short span of time.

### 11. Conclusions

In the present study, the photocatalytic degradation of Quinalphos pesticide was successively achieved using a ZnO/MgO and ZnO/SnO<sub>2</sub> nanocomposite photocatalyst. Both synthesised nanocomposites were characterised by FT-IR, XRD, UV-DRS, SEM, and EDX spectral analysis. Furthermore, the photocatalytic performance of the prepared nanocomposites for the eradication of the pesticide contaminant was

compared, and the effect of catalyst dosage, pesticide concentration, and pH were investigated. However, the ZnO/SnO<sub>2</sub> nanocomposite degraded the pesticide more effectively than the ZnO/MgO nanocomposite because of the improvement in the separation of charge carriers and other enhanced optical properties. Moreover, both nanocomposites could be regenerated and reused. The cycling ability (multiple times) indicated that the ZnO/SnO<sub>2</sub> nanocomposite was photocatalytically stable, and the rate of degradation was unaffected when compared to that of the ZnO/MgO nanocomposite. This investigation concluded that the ZnO/SnO<sub>2</sub> nanocomposite had the highest degradation efficiency to degrade the Quinalphos pesticide within 30 minutes of irradiation under direct sunlight. Hence, the ZnO/SnO<sub>2</sub> nanocomposite exhibited better photocatalytic activity than the ZnO/MgO nanocomposite for the treatment of wastewater and other organic contaminants present in an aqueous medium.

### Acknowledgement

The authors are thankful to the Nesamony Memorial Christian College, Marthandam, India, Ayya Nadar Janaki Ammal College, Sivakasi, India, Vellore Institute of Technology, Chennai, India, and Karunya Institute of Technology and Science, Coimbatore, India, for furnishing the necessary provision and support for this work.

### References

- [1] Subramanian, H., Krishnan, M., Mahalingam, A. (2022). Photocatalytic dye degradation and

- photoexcited anti-microbial activities of green zinc oxide nanoparticles synthesized via *Sargassum muticum* extracts. *RSC Advances*, 12(2), 985-997.  
<https://doi.org/10.1039/D1RA08196A>
- [2] Mali, H., Shah, C., Patel, D. H., Trivedi, U., Subramanian, R. B. (2022). Degradation insight of organophosphate pesticide chlorpyrifos through novel intermediate 2, 6-dihydropyridine by *Arthrobacter* sp. HM01. *Bioresources and Bioprocessing*, 9(1), 1-14.  
<https://doi.org/10.1016/j.biortech.2020.124641>
- [3] Kumar, K. D., Vyshnava, S. S., Shanthi, B. S., Bontha, R. R. (2022). In-silico analysis of the interaction of quinalphos and 2-hydroxyquinoxaline with organophosphate hydrolase and oxygenases. *Bio interface Research in Applied Chemistry*, 12, 608-17.  
<https://doi.org/10.1080/07391102.2023.2232045>
- [4] Yeganeh, M., Charkhloo, E., Sobhi, H. R., Esrafil, A., Gholami, M. (2022). Photocatalytic processes associated with degradation of pesticides in aqueous solutions: Systematic review and meta-analysis. *Chemical Engineering Journal*, 428, 130081.  
<https://doi.org/10.1016/j.cej.2021.130081>
- [5] Mehta, M., Sharma, M., Pathania, K., Jena, P. K., Bhushan, I. (2021). Degradation of synthetic dyes using nanoparticles: a mini-review. *Environmental Science and Pollution Research*, 28, 49434-49446.  
<https://doi.org/10.1007/s11356-021-15470-5>
- [6] Qu, T., Yao, X.X, Owens, G., Gao, L., Zhang, H. (2022) A Sustainable natural clam Shell derived photocatalyst for the effective adsorption and photo degradation of organic dyes, *Scientific Reports*, 12, 1-14.  
<https://doi.org/10.1038/s41598-022-06981-3>
- [7] Su, F., Li, P., Huang, P., Gu, M., Liu, Z., Xu, Y. (2021). Photocatalytic degradation of Organic dye and tetracycline by ternary Ag<sub>2</sub>O/AgBr-CeO, photocatalyst under visible light irradiation, *Scientific Reports*, 11, 1-13.  
<https://doi.org/10.1038/s41598-020-76997-0>
- [8]. Vedhantham, K., Girigoswami, A., Harin, A., Gringoswami, K. (2022). Waste water remediation using nano technology - A review, *Bio Interface Research in Applied Chemistry*, 12, 4476-4495.  
<https://doi.org/10.33263/BRIAC124.44764495>
- [9] Othman, Z., Sinopoli, A., Mackey, H. R., Mahmoud, K. A. (2021). Efficient Photocatalytic Degradation of Organic Dyes by AgNPs/TiO<sub>2</sub>/Ti<sub>3</sub>C<sub>2</sub>T x MXene Composites under UV and Solar Light. *ACS Omega*, 6(49), 33325-33338.  
<https://doi.org/10.1021/acsomega.1c03189>
- [10] Abouseada, N., Ahmed, M.A., Elmahgary, G. (2022). Synthesis and characterisation of novel magnetic nano articles for photo degradation of indigo carmine dye, *Materials Science for Energy Technologies*, 5, 116-124.  
<https://doi.org/10.1016/j.mset.2022.01.001>
- [11] Bano, K., Susheel, K.M., Singh, P.P., Kaushal, S. (2021). Sunlight driven photocatalytic degradation of organic pollutants using a MnVO<sub>6</sub>/BiVO<sub>4</sub> hetero junction: Mechanistic perception and degradation path ways, *Nano Scale Advances*, 22, 1-28.  
<https://doi.org/10.1039/d1na00499a>
- [12] Qutub, N., Singh, P., Sabir, S., Sagadevan, S., Oh, W. C. (2022). Enhanced photocatalytic degradation of Acid Blue dye using CdS/TiO<sub>2</sub> nanocomposite. *Scientific Reports*, 12(1), 5759.  
<https://doi.org/10.1038/s41598-022-09479-0>
- [13] Helmy, E. T., El Nemr, A., Mousa, M., Arafa, E., Eldafrawy, S. (2018). Photocatalytic degradation of organic dyes pollutants in the industrial textile wastewater by using synthesized TiO<sub>2</sub>, C-doped TiO<sub>2</sub>, S-doped TiO<sub>2</sub> and C, S co-doped TiO<sub>2</sub> nanoparticles. *Journal of Water and Environmental Nanotechnology*, 3(2), 116-127.  
<https://doi.org/10.22090/JWENT.2018.02.003>
- [14] Gola, D., Bhatt, N., Bajpai, M., Singh, A., Arya, A., Chauhan, N., Agrawal, Y. (2021). Silver nanoparticles for enhanced dye degradation. *Current Research in Green and Sustainable Chemistry*, 4, 100132.  
<https://doi.org/10.1016/j.crgsc.2021.100132>
- [15] Verma, N., Jagota, V., Alguno, A. C., Alimuddin, Rakhra, M., Kumar, P., Dugbakie, B. N. (2022). Characterization of fabricated gold-doped ZnO nanospheres and their use as a photocatalyst in the degradation of DR-31 dye. *Journal of Nanomaterials*, 2022, 1-8.  
<https://doi.org/10.1155/2022/7532332>

- [16] Joshi, N. C., Gururani, P., Gairola, S. P. (2022). Metal oxide nanoparticles and their nanocomposite-based materials as photocatalysts in the degradation of dyes. *Bio interface Research in Applied Chemistry*, 12, 6557-6579.  
<https://doi.org/10.33263/BRIAC125.65576579>
- [17] Chani, M. T. S., Khan, S. B., Rahman, M. M., Kamal, T., Asiri, A. M. (2022). Sunlight assisted photocatalytic dye degradation using zinc and iron based mixed metal-oxides nanopowders. *Journal of King Saud University-Science*, 34(3), 101841.  
<https://doi.org/10.1016/j.jksus.2022.101841>
- [18] Ahuja, P., Ujjain, S.K., Kanojia, R., Attri, P. (2021). Ahuja, P., Ujjain, S. K., Kanojia, R., Attri, P. (2021). Transition metal oxides and their composites for photocatalytic dye degradation. *Journal of Composites Science*, 5(3), 82. <https://doi.org/10.3390/jcs5030082>
- [19] Khan, N.A., Saeed, K., Khan, I., Gul, T., Sadiq, M., Uddin, A., Ivarzekker. (2022). Efficient photodegradation of Orange II dye by nickel oxide nanoparticles and nano clay supported nickel oxide nano composite, *Applied Water Science*, 12, 1-10.  
<https://doi.org/10.1007/s13201-022-01647-x>
- [20] Mathiarasu, R.R., Manikandan, A., Paneerselvam, K., George, M., Raja, K.K. (2021). Photocatalytic degradation of reactive anionic dyes RB5, RR198 and RY145 Via rare earth elements (REE) Lanthanum Substituted CaTiO<sub>3</sub> perovskite Catalysts, *Journal of Materials Research and Technology*, 15, 5936-59471.  
<https://doi.org/10.1016/j.jmrt.2021.11.047>
- [21] Lim, H., Yusuf, M., Song, S., Park, S., Park, K. H. (2021). Efficient photocatalytic degradation of dyes using photo-deposited Ag nanoparticles on ZnO structures: simple morphological control of ZnO. *RSC Advances*, 11(15), 8709-8717.  
<https://doi.org/10.1039/D0RA10945B>
- [22] Li, C., Li, H., He, G., Lei, Z., Wu, W. (2021). Preparation and photocatalytic performance of ZnO/Sepiolite composite materials. *Advances in Materials Science and Engineering*, 2021, 1-17.  
<https://doi.org/10.1155/2021/5357843>
- [23] Kaur, P., Bansal, P., Sud, D. (2013). Hetero structured nano photocatalyst for degradation of Organophosphate pesticides from aqueous streams, *Journal of the Korean Chemical Society*, 57, 382-388.  
<http://dx.doi.org/10.5012/jkcs.2013.57.3.382>
- [24] Jiang, S., Lin, K., Cai, M. (2020). ZnO nanomaterials: Current advancements in antibacterial mechanisms and applications, *Frontiers in Chemistry*, 8, 1-5.  
<https://doi.org/10.3389/fchem.2020.00580>
- [25] Krishnan, B., Velavan, R., Batoo, K.M., Raslan, E.H. (2020). Microstructure, optical and photocatalytic properties of MgO nanoparticles, *Results in Physics*, 16, 1-4.  
<https://doi.org/10.1016/j.rinp.2020.103013>
- [26] Paramarta, V., Taufik, A., Munisa, L., Saleh, R. (2017, January). Sono- and photocatalytic activities of SnO<sub>2</sub> nanoparticles for degradation of cationic and anionic dyes. In *AIP Conference Proceedings* (Vol. 1788, No. 1). AIP Publishing.  
<https://doi.org/10.1063/1.4968378>
- [27]. Sraw, A., Kaur, T., Pandey, Y., Verma, A., Sobti, A., Wanchoo, R. K., Toor, A. P. (2020). Photocatalytic degradation of monocrotophos and quinalphos using solar-activated S-doped TiO<sub>2</sub>. *International journal of Environmental Science and Technology*, 17, 4895-4908.
- [28] Behera, L., Barik, B., Mohapatra, S. (2021). Improved photodegradation and antimicrobial activity of hydrothermally synthesized 0.2 Ce-TiO<sub>2</sub>/RGO under visible light. *Colloids and Surfaces A: Physicochemical and Engineering Aspects*, 620, 126553.  
<https://doi.org/10.1016/j.colsurfa.2021.126553>
- [29] Garg, R., Gupta, R., Singh, N., Bansal, A. (2022). Eliminating pesticide quinalphos from surface waters using synthesized GO-ZnO nanoflowers: Characterization, degradation pathways and kinetic study. *Chemosphere*, 286, 131837.  
<https://doi.org/10.1016/j.chemosphere.2021.131837>
- [30] Sharotri, N., Sharma, D., Sud, D. (2019). Experimental and theoretical investigations of Mn-N-co-doped TiO<sub>2</sub> photocatalyst for visible light induced degradation of organic pollutants. *Journal of Materials Research and Technology*, 8(5), 3995-4009.

- <https://doi.org/10.1016/j.jmrt.2019.07.008>
- [31] Fernandez, A.S., Garcia, S.C., Villalba, L.S., Cornelio, S.G., Rabanal, M.E., Fort, R., Quintana, P. (2017). Synthesis, photocatalytic and antifungal properties of MgO, ZnO and Zn/Mg oxide nanoparticles for the protection of calcareous stone heritage, *Applied Materials and Interfaces*, 9, 24873-24886.  
<https://doi.org/10.1021/acsami.7b06130>
- [32] Sangeetha, M., Karthick, K.V., Ravishankar, R., Anantharaju, K.S., Nagabhushana, H., Jeetendra, K., Vidya, Y.S., Renuka, L. (2017). Synthesis of ZnO, MgO and ZnO/MgO by solution combustion method: Characterisation and photocatalytic studies, *Materials today: Proceedings*, 4, 11791-1179.  
<https://doi.org/10.1016/j.matpr.2017.09.096>
- [33] Zarei, S., Hasheminasari, M., Masoudpanah, S. M., Javadpour, J. (2022). Photocatalytic properties of ZnO/SnO<sub>2</sub> nanocomposite films: role of morphology. *Journal of Materials Research and Technology*, 17, 2305-2312.  
<https://doi.org/10.1016/j.jmrt.2022.01.126>
- [34] Verma, N., Yadav, S., Mari, B., Mittal, A., Jindal, J. (2018). Synthesis and characterization of coupled ZnO/SnO<sub>2</sub> photocatalysts and their activity towards degradation of cibacron red dye. *Transactions of the Indian Ceramic Society*, 77(1), 1-7.  
<https://doi.org/10.1080/0371750X.2017.1417059>
- [35] Das, S., Srivasatava, V. C. (2016). Synthesis and characterization of ZnO-MgO nanocomposite by co-precipitation method. *Smart Science*, 4(4), 190-195.  
<https://doi.org/10.1080/23080477.2016.1260425>
- [36] Lin, L., Han, Y., Fuji, M., Endo, T., Wang, X., Takahashi, M. (2008). Synthesis of hexagonal ZnO microtubes by a simple soft aqueous solution method. *Journal of the Ceramic Society of Japan*, 116(1350), 198-200.  
<https://doi.org/10.2109/jcersj2.116.198>
37. Sutapa, I. W., Wahab, A. W., Taba, P., La Nafie, N. (2018). Synthesis and structural profile analysis of the MgO nanoparticles produced through the sol-gel method followed by annealing process. *Oriental Journal of Chemistry*, 34(2), 1016.  
<http://dx.doi.org/10.13005/ojc/340252>
- [38] Sumathi. P. (2020). Synthesis and characterisation of SnO<sub>2</sub> nanocomposite against bacteria and fungi, *International Journal of Chemtech Research*, 13(3), 203-209.  
<https://doi.org/10.20902/IJCTR.2019.130317>
- [39] Yar, A., Haspulat, B., Üstün, T., Eskizeybek, V., Avcı, A., Kaniş, H., Achour, S. (2017). Electrospun TiO<sub>2</sub>/ZnO/PAN hybrid nanofiber membranes with efficient photocatalytic activity. *RSC Advances*, 7(47), 29806-29814.  
<https://doi.org/10.1039/C7RA03699J>
- [40] Sinha, A. K., Pradhan, M., Sarkar, S., Pal, T. (2013). Large-scale solid-state synthesis of Sn-SnO<sub>2</sub> nanoparticles from layered SnO by sunlight: a material for dye degradation in water by photocatalytic reaction. *Environmental Science and Technology*, 47(5), 2339-2345.  
<https://doi.org/10.1021/es303413q>
- [41] Kajbafvala, A., Ghorbani, H., Paravar, A., Samberg, J. P., Kajbafvala, E., Sadrnezhaad, S. K. (2012). Effects of morphology on photocatalytic performance of Zinc oxide nanostructures synthesized by rapid microwave irradiation methods. *Superlattices and Microstructures*, 51(4), 512-522.  
<https://doi.org/10.1016/j.spmi.2012.01.015>
- [42] Kiwaan, H. A., Atwee, T. M., Azab, E. A., El-Bindary, A. A. (2020). Photocatalytic degradation of organic dyes in the presence of nanostructured titanium dioxide. *Journal of Molecular Structure*, 1200, 127115.  
<https://doi.org/10.1016/j.molstruc.2019.127115>
- [43] Pachiyappan, J., Gnanasundaram, N., Rao, G. L. (2020). Preparation and characterization of ZnO, MgO and ZnO-MgO hybrid nanomaterials using green chemistry approach. *Results in Materials*, 7, 100104.  
<https://doi.org/10.1016/j.rinma.2020.100104>
- [44] Subhan, M. A., Ahmed, T., Uddin, N., Azad, A. K., Begum, K. (2015). Synthesis, characterization, PL properties, photocatalytic and antibacterial activities of nano multi-metal oxide NiO·CeO<sub>2</sub>ZnO. *Spectrochimica Acta Part A: Molecular and Biomolecular Spectroscopy*, 136, 824-831.  
<https://doi.org/10.1016/j.saa.2014.09.100>
- [45] Kathik, K., Dhanushkodi, S., Gobinath, C., Prabukumar, S., Sivaramakrishnan, S. (2019). Ultrasonic-assisted CdO-MgO nanocomposite

- for multifunctional applications, *Materials Technology*, **34**, 403-414.  
<https://doi.org/10.1080/10667857.2019.1574963>
- [46] Jin, C., Ge, C., Jian, Z., Wei, Y. (2016). Facile synthesis and high photocatalytic degradation performance of ZnO/SnO<sub>2</sub> hollow Spheres, *Nano Scale Research Letters*, **11**, 1-6.  
<https://doi.org/10.1186/s11671-016-1740-y>
- [47]. Ali, A. M., Qreshah, O., Ismail, A. A., Harraz, F. A., Algarni, H., Assiri, M. A., Chiu, W. S. (2019). Morphological and optical properties of SnO<sub>2</sub> doped ZnO nanocomposites for electrochemical sensing of hydrazine. *International Journal of Electrochemical Science*, **14**(2), 1461-1478.  
<https://doi.org/10.20964/2019.02.04>
- [48]. Dulta, K., Koşarsoy Ağçeli, G., Chauhan, P., Jasrotia, R., Chauhan, P. K., Ighalo, J. O. (2022). Multifunctional CuO nanoparticles with enhanced photocatalytic dye degradation and antibacterial activity. *Sustainable Environment Research*, **32**(1), 1-15.  
<https://doi.org/10.1186/s42834-021-00111-w>
- [49]. Adeel, M., Saeed, M., Khan, I., Muneer, M., Akram, N. (2021). Synthesis and characterization of Co-ZnO and evaluation of its photocatalytic activity for photodegradation of methyl orange. *ACS Omega*, **6**(2), 1426-1435.  
<https://doi.org/10.1021/acsomega.0c05092>
- [50]. Amdeha, E., Mohamed, R. S. (2021). A green synthesized recyclable ZnO/MIL-101 (Fe) for Rhodamine B dye removal via adsorption and photo-degradation under UV and visible light irradiation. *Environmental Technology*, **42**(6), 842-859.  
<https://doi.org/10.1080/09593330.2019.1647290>